



# Nonlinear fiber effects in ultra-high power $10 \times 10$ Gbit/s WDM-IM free-space systems for satellite links

ERNESTO CIARAMELLA\*  AND GIULIO COSSU 

*Scuola Superiore Sant'Anna, Istituto TeCIP, Pisa, Italy*

\**e.ciaramella@santannapisa.it*

**Abstract:** We investigate an unexplored type of nonlinear impairments that will take place in a very short fiber after the booster amplifier in a Free Space Optical (FSO) system for space communications. In Earth-satellite links, optical power levels up to 100 W could be required at the transmitter side to achieve the foreseen 100 Gbit/s capacity, because of the extremely high losses. These systems thus need an optical booster amplifier having very high optical power and it should be connected to the transmitting telescope by means of a short fiber (few meters). Here, we discuss and investigate the impact of the nonlinear fiber effects by means of numerical simulations, and estimate the impairments in a Wavelength Division Multiplexing (WDM)  $10 \times 10$  Gbit/s system with intensity modulation. The obtained results clearly indicate that, in this system, the most relevant effect is Four Wave Mixing. We proved that this can be observed as soon as the total power exceeds 20 W. Due to the short fiber length, the system impairments are not affected by chromatic dispersion or channel spacing. We demonstrate that an effective means to reduce the impact is by adopting Polarization Interleaving, i.e., odd and even channels with orthogonal state of polarization. This solution could not work in long terrestrial links because of polarization mode dispersion, yet it can be effectively exploited in short fiber patch cords. These results can be used as a guideline to control this type of impairment in high-power FSO systems for satellite links.

© 2024 Optica Publishing Group under the terms of the [Optica Open Access Publishing Agreement](#)

## 1. Introduction

FUTURE high-speed wireless communications for intersatellite and feeder (Earth-satellite) links will be based on Free Space Optical (FSO) systems [1–3]. A paramount example is the design analysis of the Hydron network [4], proposed by the European Space Agency, which will combine FSO technology with Wavelength Division Multiplexing (WDM) to reach  $\geq 100$  Gbit/s total capacity [5].

It is widely expected that most of the WDM-FSO technology can leverage upon optical fiber communications devices and subsystems, combined with proper telescopes and accurate pointing solutions. However, the power budget analysis shows that much higher power levels than in terrestrial links should be required for space links [6]. These high values are frequently proposed because FSO links usually have no nonlinear effects. Among the various FSO satellite links, the feeder links typically require the highest power values, because they suffer from the impairments due to atmospheric conditions and they also involve the longest distances. This is particularly critical in very-high throughput links, e.g., 100 Gbit/s, where we could need very high-power levels, i.e. several tens of Watts [7]. Noteworthy, the maximum output power of present commercial amplifiers is around few Watts, hence this need is pushing the research towards the realization of ultra-high power optical amplifiers (UHPOA) [8]: to reach this goal, various solutions were recently demonstrated that achieve output powers largely exceeding 10 W [9,10].

Although the largest portion of the signal path is in free-space, system design studies should carefully consider the nonlinear impairments. Recently, this topic is becoming apparent [9,11]: as an example, it is now clear that a few meters of fibers will be needed to connect the output of the UHPOA to the transmitting telescope [8]. Furthermore, nonlinear effects can also take place in the UHPOA, either in the active fiber or in short pigtails of the passive components. The last are, however, very specific to be predicted, because they depend on the type of active fiber, pumping scheme, and gain coefficient (in the very last part of the UHPOA, where the optical power is the highest).

Noteworthy, in an EDFA, we would see a mirrored condition in respect of common fibers: along fibers, the signal power decreases exponentially, and the first section of the link (effective length,  $L_{eff}$ ) is the most important for nonlinear effects [12]. Along the EDFA active fiber, the power increases, therefore, we should rather consider the final section, where we must know the gain coefficient to correctly estimate the impact of nonlinearities. As an example, if we had 1 dB/m of gain in the final part of the amplifier, we would get an equivalent effective length of around 4 m (a different gain coefficient would give a different length and a different impact of nonlinearities). This figure is not affected by the total length of the active fiber, because most of the nonlinear effects would take place in the last few meters of amplifier.

Moreover, it is expected that other short pieces of common fiber can be present in the UHPOA, after the active fiber (as example, it is unlikely that the UHPOA output connector will be made just on the active fiber itself): these pieces of fiber will have a similar impact as the one that is considered in the following. The nonlinear coefficient in the active fiber also plays a key role. Unfortunately, all those details are very particular and are strictly related to developments, which are still in progress: however, the results given in the following can be readily extended to any amplifier, once the above parameters are known, by exploiting basic scaling laws of nonlinear effects in optical fibers [12]. This can also help to optimize the design of future UHPOAs.

In all cases, we note that the length of the involved fibers (few meters) is around four orders of magnitude lower than the usual  $L_{eff}$  value in terrestrial optical fiber links (around 20 km) [12]; however, this is unfortunately counter-balanced by the huge power levels. Given the extremely short length of the fiber, we expect remarkable difference from nonlinear impairments in terrestrial fiber links: namely, both attenuation and dispersion effects are negligible. Indeed, the well-known quantities, referred as walk-off length [13] and phase matching length [14], would be much longer than the nonlinear effective length [12]: thus, we expect relevant phenomena due to both Cross-Phase Modulation (XPM) and Four Wave Mixing (FWM) [12]-[14]. Self-Phase Modulation (SPM) would also take place. However, both SPM and XPM do not affect intensity-modulated (IM) signals thanks to the low accumulated dispersion, whilst they can directly impair phase-modulated signals. Finally, we note that WDM signals will likely experience also cross-polarization modulation: however, this can only affect polarization-multiplexed signals, which require coherent detection and are not considered in the following. Therefore, for the same number of channels and same capacity, we expect FWM to be the most relevant effect in Intensity Modulation with Direct Detection (IM-DD) systems.

The role of FWM was also indicated as predominant in a project report, publicly available [15], which also included an estimation of the impact of the nonlinear effects into a UHPOA. In this report, the authors observed that FWM represents a significant limitation in WDM systems with five channels (either intensity- or phase-modulated signals), when they were amplified by a newly developed high-power booster. Unfortunately, details on the used booster were not given and are not public, hence it is difficult to extract the relevant information to apply in a different condition. Therefore, a new and more detailed analysis was necessary.

In this paper, we examine the impact of nonlinear optical effects in a short fiber, specifically a patch cord that will be utilized in FSO systems for space links. To our knowledge, this is the first systematic investigation of power limitations due to nonlinear effects in FSO links. In

order to restrict the analysis to a practical configuration, we make some key assumptions. As IM-DD is simple to deploy, and has quicker recovery time after the (frequent) fading events typical of FSO links [16] we consider here this type of format: in fiber communications, the most common IM-DD systems are at 10 Gbit/s, with Non Return to Zero (NRZ) format. Since 100 Gbit/s aggregate capacity is frequently assumed as the first capacity target [4], we thus consider a  $10 \times 10$  Gbit/s system.

Finally, we model a patch cord made of common single-mode fiber (SMF, G.652) of  $L = 3$  m length. Under the previous assumptions, numerical simulations were performed to verify that the dominating effect is FWM among the channels. Thus, we determine the power values for which the nonlinear effects become relevant in the worst-case condition. Finally, we determine that this limit can be overcome by properly setting the State of Polarization (SoP) of the channels.

We highlight that the paper concerns nonlinear Kerr effects. As known, other nonlinear effects can take place in optical fibers. Namely, Stimulated Brillouin Scattering (SBS) is often indicated as the one occurring at lowest intensity levels, as its threshold value ( $P_{th}$ ) in a SMF is around 10 mW for NRZ signals (see Fig. 2 in [17]). As SBS is a single-channel type of effect, the previous  $P_{th}$  is given as power/channel in WDM systems; furthermore, in a typical fiber system, it corresponds to a nonlinear effective length of around 20 km (SBS threshold is the same in single span and multi-span links). Therefore, simple scaling for 3 m-long fiber gives  $P_{th}$  of around 70 W/channel: we note that this figure can be also estimated by the equation for a modulated signal  $P_{th} = 2P_{th}^{CW} = 84 A_{eff} / (g_B L_{eff})$  where  $A_{eff} = 100 \mu\text{m}^2$ ,  $g_B = 4 \cdot 10^{-11}$  m/W, and  $L_{eff} = 3$  m (for very short fibers  $L_{eff} = L$ ) [17]. Hence, as we have 10 WDM channels, we get a huge total power, of around 700 W, i.e. quite above the highest achievable values. The other category of nonlinear effects is Stimulated Raman Scattering (SRS), which has threshold given in terms of total power. However, due to the much lower gain coefficient,  $g_R$ , SRS threshold is much higher than SBS threshold: it is indeed around 600 mW in a long fiber. Simple estimations, based on the ratio of effective lengths, indicate a SRS threshold of around 5 MW for the considered short patchcord (again this figure can be calculated by the equation  $P_{th}^R = 42 A_{eff} / (g_R L_{eff})$  where now  $g_R \approx 1 \cdot 10^{-13}$  m/W [12]). Indeed, we are going to discuss a total output power lower up to 70 W: in that case, these effects should not be relevant. Indeed, neither SBS nor SRS were observed in a recent WDM experiment at 50 W total power [10]. Hence both SBS and SRS will not be addressed in the following.

## 2. Model and results

We realized a software tool that was used to extensively investigate the transmission performance in a  $10 \times 10$  Gbit/s FSO system. A schematic of the system is presented in Fig. 1.

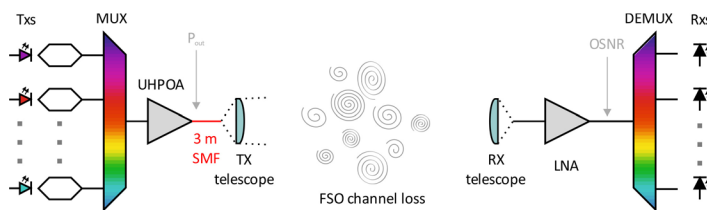


**Fig. 1.** Schematic of the FSO link. The WDM signals are wavelength-multiplexed (MUX), then they are amplified by an ultra-high power optical amplifiers (UHPOA) with  $P_{out}$  total power. This will be input of a 3-m patch cord and finally reach the TX telescope. At the RX side, light is amplified by a Low Noise Amplifier (LNA), the channels are demultiplexed (DEMUX), and then each of them is detected by an RX.

Each WDM channel is NRZ-coded using a chirp free modulator (bandwidth 10 GHz); the bit sequence (65536 bits) is made of an equal number of marks and spaces produced by a

random generator; for each channel, the bit-sequence is independently generated and randomly time-shifted. Optical signals can be multiplexed so that the even and the odd channels can have either the same polarization (aligned SoPs) or orthogonal states (alternate SoPs) at the UHPOA input. We assume that the total output power of the UHPOA ( $P_{out}$ ), which is also the power at the input of the patchcord, is equally distributed over the 10 channels.

Channel spacing ( $\Delta\nu$ ) is initially set at 100 GHz: as we will see later, this parameter has no impact on the nonlinear effects, since the patch cord fiber is a very short ( $L = 3$  m) SMF. The nonlinear coefficient for average polarization is  $1.4$  (W·km) $^{-1}$ , typical of common SMFs. Attenuation is 0.2 dB/km and chromatic dispersion is 16 ps/nm/km. Thanks to its short length neither dispersion nor attenuation effects are expected to be significant [12]. We simulate the nonlinear propagation in the fiber by means of the split-step Fourier method, solving the coupled nonlinear equations (Eqns. 6.2.1 and 6.2.2 in [12]). Due to its short length, along the patch cord the propagation of light can be described by means of a single waveplate model [12].

We note that a wide literature exists on the coupled Nonlinear Schroedinger Equations (NLSEs) accounting for polarization effects. Different formulations can be given, either considering as a base a pair of linear polarizations (e.g., x and y) or the two circular polarizations (clockwise and counter-clockwise). In our case, the simulator solves the following coupled NLSEs for two circular SoPs (these are derived from Eqns.6.1.15 and 6.1.16 in [12], neglecting the low-birefringence and changing variables as in Ch.2 in [12], to remove the  $\beta_1$  term):

$$\begin{aligned}\frac{\partial A_+}{\partial z} &= i\gamma\frac{2}{3}(|A_+|^2 + 2|A_-|^2)A_+ - i\frac{\beta_2}{2}\frac{\partial^2 A_+}{\partial t^2} - \frac{\alpha}{2}A_+ \\ \frac{\partial A_-}{\partial z} &= i\gamma\frac{2}{3}(|A_-|^2 + 2|A_+|^2)A_- - i\frac{\beta_2}{2}\frac{\partial^2 A_-}{\partial t^2} - \frac{\alpha}{2}A_-\end{aligned}$$

where the nonlinear Kerr coefficient is  $\gamma=1.4$  (W km) $^{-1}$ , the chromatic dispersion coefficient is  $\beta_2=-20.3$  ps $^2$ /km (corresponding to  $D = 16$  ps/nm/km), and the loss coefficient is  $\alpha=-0.05$  km $^{-1}$ . Note that  $A_+$  and  $A_-$  are linear combinations of the field components along x and y-axis. As well-known, the above equations do not explicitly show the familiar FWM term: this can only be obtained by writing down the two terms  $A_+$  and  $A_-$ , which are related to the components (+ or -) of the field of all WDM channels (a full derivation is out of the scope of this paper, but, as example, a similar derivation, in the simpler condition of the scalar NLSE, can be found in [21]). After the fiber, the channel is then modelled as pure attenuation.

We simulated a simple configuration where the signal from the patchcord is sent over free-space, undergoes a variable loss (quite high) and then enters a pre-amplifier. The optical pre-amplifier (LNA) has noise figure  $n_F = 4$  dB. Before detection, each channel is optically filtered with a 20 GHz bandwidth Gaussian filter. The RX has an ideal photodiode followed by a 4<sup>th</sup> order Bessel filter (7.5 GHz bandwidth) and usual clock and data recovery (CDR). The received signal is sampled at the center of the eye diagram and then, the received bit-sequence is extracted from the samples, by applying the optimal decision threshold [18].

Finally, we estimate the pre-FEC BER value by directly comparing the received to the transmitted bit sequence.

Since the pre-amplifier has typical gain of 30 dB or higher, the performance of the system is not significantly affected by any other noise source, but it only depends on the degradation of the optical signal to noise ratio (OSNR) [19]. As today all WDM systems implement Forward Error Correction (FEC), we will consider as a target BER the value that corresponds to the typical threshold of pre-FEC BER value, i.e.,  $10^{-3}$ .

We note that, in our model, we use some simplifying assumptions to have a clear view of the effect of the nonlinear impairments. First, we only model the nonlinear effects in the external patch cord, and do not include the effect of nonlinear propagation in the amplifier itself (due to the active fiber and any other internal fiber pigtails), as explained above. However, the obtained results can be a useful guideline and they are quite general, so that they can be extended with

minor effort also to include these other cases once the specific parameters of the UHPOA are known.

In our simulation, we assume a stable FSO loss; actually, the FSO channel is not exactly stationary, however it is well known that it has a fixed loss over a finite coherence time, typically around several milliseconds [20]. Therefore, the effects that we are investigating here refer to that specific time window, when loss is fixed. Under these conditions, the instantaneous pre-FEC BER is determined only by the OSNR value at the output of the RX [18], as usual in fiber links. Thus, the OSNR value needed to reach the pre-FEC BER value is a key general system parameter (actually, depending on the system details this can be used to design the system in terms of instantaneous or, by proper scaling, average power at the RX) [19]. Indeed, in order to perform a complete system analysis, these results should be averaged over statistical fluctuations, which would require a specific mathematical investigation to determine the outage probability as function of average received OSNR. This complete analysis is presently out of scope of this paper: however, the penalty results reported in the following allow to determine how the required OSNR would scale when the system is affected by nonlinear effects.

Since FWM is known to depend on the relative SoP among the channels [12], initially we took the worst-case condition, i.e., all channels having the same SoP. To make the simulation more realistic, the channels are not precisely spaced at 100 GHz, but rather randomly detuned by a very small amount (<1 GHz).

First, we analyzed the signal at the output of the UHPOA patchcord. We observed that relevant nonlinear impairments arise even when  $P_{out}$  is much lower than 100 W: as an example, in Fig. 2(a-b), we show the normalized eye diagrams taken at the output of the patch cord, for the central channel, where no optical nor electrical noise is added, for two quite different regimes. The eye diagram in Fig. 2 (a) was taken at  $P_{out} = 1$  W, whilst in Fig. 2 (b) was taken at  $P_{out} = 40$  W. The apparent source of signal degradation are nonlinear effects. Clearly, the impairments cannot be ascribed to XPM: although XPM is surely present, it cannot be the real problem, because we are using Direct Detection, and there is no way that phase modulation can become intensity distortion [13] (there is no chromatic dispersion in free space, with negligible contribution by the patchcord itself). As another option, XPM might also produce penalties if the induced spectral broadening can interplay with very narrow filters. In our case, however, we have wide optical filters (20 GHz FWHM), thus this would require a huge spectral broadening to see any relevant effect.

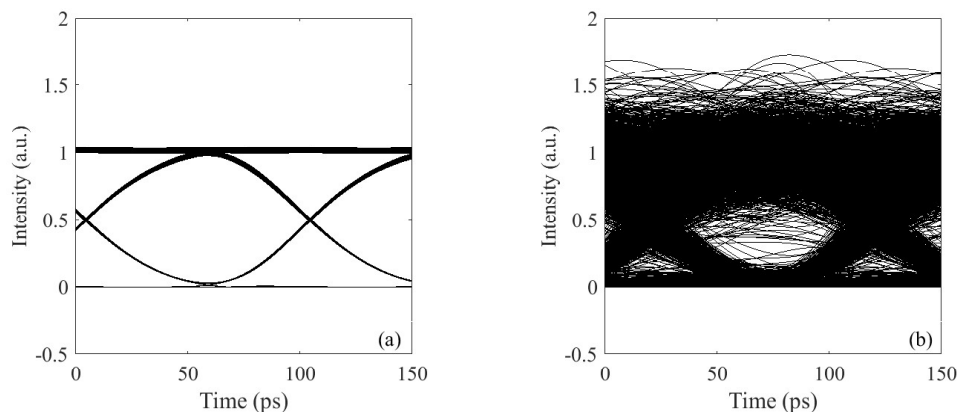


**Fig. 2.** Eye diagrams for the central WDM channel for  $P_{out} = 1$  W (a) and 40 W (b).

On the other hand, the emergence of FWM can be clearly observed in the output spectra. To this aim, in Fig. 3, we report the optical spectra taken at the input (a) and output (b) of the patch



cord for  $P_{out} = 40$  W: as we can see, this directly confirms that FWM is the key issue. Several FWM products are visible here, with a power level approximately -20 dB lower than the signals: this is significantly above the well-known maximum acceptable FWM-crosstalk value, typically assumed to be -23 dB [14,22].

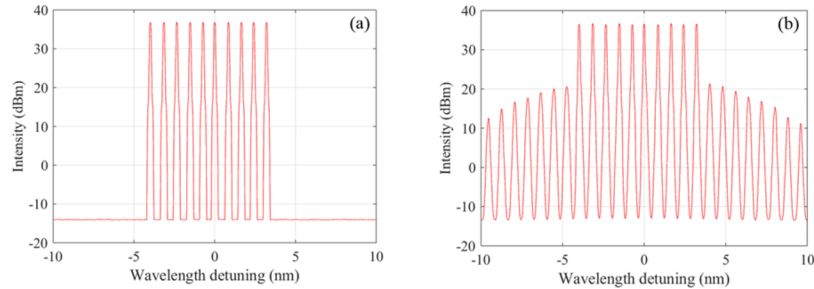


**Fig. 3.** Optical spectra taken at patch cord input (a) and output (b) (res. bw = 0.1 nm) assuming  $P_{out} = 40$  W.

In order to have a quantitative estimation of the impact of this effect, we then conducted a numerical investigation on the system performance. As described above, the performance is determined by the OSNR, depending on nonlinear distortion, signal power at the pre-amplifier and the noise figure [19]. Furthermore, as this system will make use of FEC, we should be concerned with the  $OSNR_{req}$ , i.e., the OSNR value that is needed to attain the FEC threshold (maximum BER that FEC can correct), as defined in [19].

The results were practically obtained by varying the FSO loss: however, for the sake of clarity, they are reported as function of the OSNR value after the pre-amplifier. Then, we define an OSNR-penalty as the difference in  $OSNR_{req}$ , i.e., the value needed to achieve the pre-FEC BER of  $10^{-3}$  [18].

To this aim, different BER curves are obtained at different values of  $P_{out}$  and variable loss. As an example, we report in Fig. 4(a) the BER curve versus OSNR for two  $P_{out}$  values, i.e., 5 W (circles), and 40 W (red squares), for the worst-case condition of aligned SoPs. Since we have  $10^{-3}$  pre-FEC BER threshold, we see that 40 W power has error floor, infinite OSNR penalty compared to 5 W: this eliminates the 9-dB benefit in terms of power budget that we would obtain in a linear condition when increasing  $P_{out}$  from 5 to 40 W.

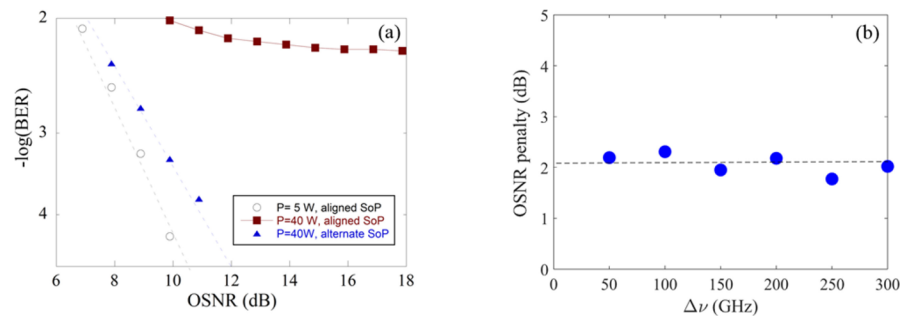


**Fig. 4.** Estimated BER curve vs. OSNR for the central WDM channel (a): the three curves refer to low power (5 W, circles, with parallel SoPs) 40 W with either parallel SoPs (red squares) or alternate SoPs (blue triangles); in (b), we present the dependence of OSNR-penalty at pre-FEC BER vs. channel spacing at fixed power ( $P_{out} = 30$  W), dashed line represents the mean value.

As mentioned, these curves were taken in the worst-case condition, where all channels have the same SoP, and we choose the worst-case SoP. Conversely, a system where odd and even channels have orthogonal SoPs corresponds to the best case. Therefore, we conducted a simulation under the optimal conditions and indeed obtained that alternate SoPs significantly reduce the impairments, with a penalty down to about 0.5 dB at 40 W (blue triangles).

As the system is affected by FWM, it might be argued that we could improve the performance by increasing the channel spacing  $\Delta\nu$ . To confirm that this is not the case, we run simulations at 30 W, with various  $\Delta\nu$  values. The results are reported in Fig. 4(b), in terms of OSNR penalty, as defined above. As we can see, there is no significant difference among the various cases, within the estimated uncertainty of the final penalty. This confirms the initial expectations that channel spacing cannot help to reduce FWM.

In order to summarize the results in a comprehensive figure, we report in Fig. 5 the OSNR-penalty (at pre-FEC BER of  $10^{-3}$ ), as a function of the total transmitter power ( $P_{out}$ ). The first curve (red triangles) refers to the worst-case, when all channels have the same SoP. The second curve (blue dots) refers to the best-case, where odd and even channels have orthogonal SoPs. We see a very significant difference between the two curves; this indicates that by adopting alternate polarizations, we could transmit at least 3 dB higher power, which has relevant impact on the whole link budget.

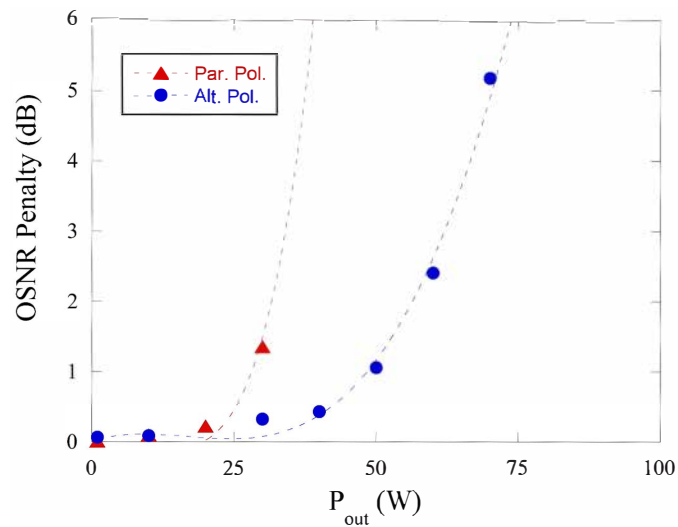


**Fig. 5.** Estimated OSNR-penalty for different total output EDFA power values, for worst-case (red triangles, all SoPs aligned) and best-case (blue dots, alternate orthogonal SoPs) scenarios.

We can comment that alternate polarizations in FSO is effective and possible thanks to the limited length of active fiber (and patch cord), this is a major difference with respect to fiber communications, where WDM signals at consecutive wavelengths will not maintain SoP orthogonality along the (long) link, because of Polarization Mode Dispersion (PMD). In our case, the quite short length of fiber patch-cord (and of the active fiber in the amplifier) allows to predict that the mutual SoP will not change.

Therefore, in our case, a polarization control could be implemented on each of the WDM channel by obtaining this condition the input of the UHPOA, with a minor power split and polarization monitor; that power splitter cannot affect the total output power, since the booster amplifier works in saturation. An alternative option could be to use transmitters with polarization maintaining fibers (PMFs) and properly rotated connectors.

Finally, it may be argued that orthogonality between odd and even channels might be an extremely critical condition and we could have a low realistic tolerance. In order to assess the real tolerance, we run a specific set of simulations and introduce a new parameter ( $\Delta\alpha$ ): in the ideal case, we assumed that all channels have linear SoP at the HPOA input, yet odd and even channels are at 90 degrees. We then rotated the SoP of even channels by the angle  $\Delta\alpha$  and estimated the corresponding OSNR penalty. The obtained results are reported in Fig. 6, where we report the OSNR penalty relative to the back-to-back condition (indeed we have 1 dB penalty at  $\Delta\alpha=0$ ); they show that around 30 degrees of  $\Delta\alpha$  tolerance is acceptable, with very limited additional degradation. This clearly indicates that the SoP orthogonality of odd and even channels is not a very strict requirement, and it can be obtained by using realistic components.

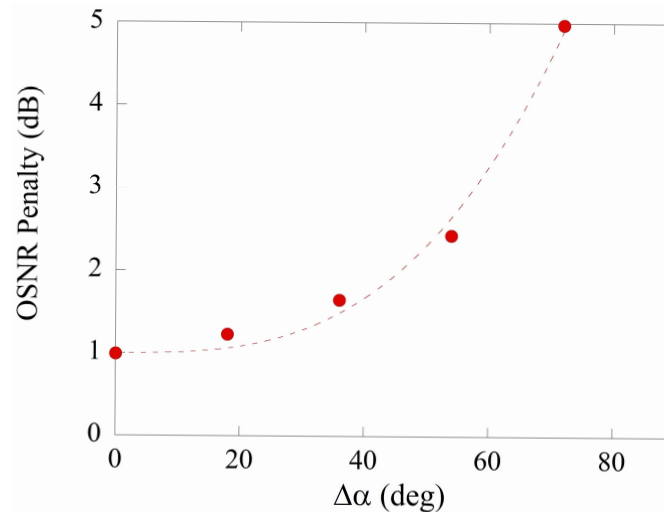


**Fig. 6.** Estimated OSNR penalty when we set alternate polarizations, but we have a deviation from perfectly orthogonality (by an angle  $\Delta\alpha$ ) among odd and even channels. The assumed power is  $P_{out} = 50$  W. The OSNR penalty is relative to the back-to-back requested OSNR, not the OSNR for  $\Delta\alpha=0$ .

Alternate polarization may not be the only solution: unequal channel spacing (UCS) may also be considered [23]. However, UCS has well-known issues of low spectral efficiency [23]. As a nonlimiting example, if we assume the ten channels to be fixed to the typical frequency grid (100 GHz), it can be seen that 10 channels will hardly fit the common EDFA bandwidth (35 nm). Thus, UCS needs lower frequency spacing (e.g. 50 GHz, for which it requires around 25 nm of bandwidth for ten channels). In the considered configuration, UCS could be a valid alternative, although it should be carefully adopted also because UHPOA are expected to have much lower bandwidth than current amplifier (as example, the bandwidth of a 50 W amplifier was 25 nm in [10]).

### 3. Conclusion

We used numerical simulations to investigate the occurrence of nonlinear effects in FSO space systems, due to the (unavoidable) presence of patch cords connecting an UHPOA to the transmitting telescope. We considered a  $10 \times 10$  Gbit/s IM-DD system, with 100 GHz spacing. Our simulations show that FWM strongly affects the performance as soon as the power exceeds 25 W, when the SoPs of all WDM channels are aligned (worst case). As the patch cord is very short, we cannot rely on wider spacing to reduce the FWM, because the phase matching length is much longer than the fiber length.



The obtained results are expected to have a significant relevance in the link budget of long-distance FSO links. It is important to note that, especially in ground-to-GEO links, huge losses are expected. As the actual loss is determined by the combination of various propagation phenomena (diffraction, scintillation, beam wandering etc.), this results into a complex problem when designing the FSO link. As different (independent) statistical variables determine the final loss, the complete statistical analysis is required to estimate the outage probability [24]. Since here we have demonstrated the role of nonlinear effects, they have also to be considered into the link design process: this will result into a significant limitation on the maximum available loss in the link, because now we have a limit to the increase of transmitter power. This is similar to what is observed in optical fiber links.

We also note that the presented analysis was restricted to IM-DD, as this is the simplest modulation format; moreover, it may also be preferred since it has much shorter recovery time after any deep fading [16] and would be affected only by FWM, in the considered configuration. We expect that the in-depth investigation of nonlinear effects in signals with other modulation formats, especially those exploiting phase modulation (either based on direct or coherent detection) be by far more complex, since those would be also impaired by XPM and cross polarization modulation. Yet, we plan to carry out this extended analysis in the near future.

Noteworthy, thanks to the short length, SoP orthogonality at consecutive wavelengths can be fixed at the input and would be maintained throughout the amplifier and patchcord: therefore, the tolerance can be strongly improved by adopting channels with alternate SoP. Around 100% higher power can be then safely transmitted.

Clearly, all the obtained values strictly depend on the patchcord length: if a shorter/longer fiber is adopted, the power values should scale accordingly: it is indeed a good approximation to assume that the total effect depends on the product  $LP_{out}$ . Therefore, since we assumed a 3 m-long patch cord, the effects that we obtained at 40 W could be expected at 30 W if the patch cord is 4 m long. Conversely, a shorter fiber could help to use much higher power values: unfortunately, we cannot expect fiber lengths much shorter than the value we assumed (3 m).

As a simple additional means to improve the tolerance, we have seen that we could use exploit also unequal channel spacing [14]. Although complex, this may represent a viable solution when we have a low number of channels; on the other side, it can strongly compromise the spectral efficiency, limiting possible future upgrades of the total number of channels, i.e., the total transmitted capacity.

**Funding.** Ministero dell'Università e della Ricerca (PE00000001 - program "RESTART&apos;&apos;).

**Disclosures.** The authors declare no conflicts of interest.

**Data availability.** No data were generated or analyzed in the presented research.

## References

1. R. De Gaudenzi, P. Angeletti, D. Petrolati, *et al.*, "Future technologies for very high throughput satellite systems," *Int. J. Satell. Commun. Netw.* **38**(2), 141–161 (2020).
2. H. Kaushal and G. Kaddoum, "Optical Communication in Space: Challenges and Mitigation Techniques," *IEEE Commun. Surv. Tutorials* **19**(1), 57–96 (2017).
3. C. M. Schieler, K. M. Riesing, B. C. Bilyeu, *et al.*, "On-orbit demonstration of 200-Gbps laser communication downlink from the TBIRD CubeSat," *Proc. SPIE* **12413**, 1241302 (2023).
4. H. Hauschildt, C. Elia, H. L. Moeller, *et al.*, "Hydron: High throughput optical network," in *2019 IEEE International Conference on Space Optical Systems and Applications (ICSOS)*, (2019), pp. 1–6.
5. E. Ciaramella, Y. Arimoto, G. Contestabile, *et al.*, "1.28 Terabit/s (32 × 40 Gbit/s) WDM Transmission System for Free Space Optical Communications," *IEEE J. Select. Areas Commun.* **27**(9), 1639–1645 (2009).
6. R. Saathof, R. D. Breeje, W. Klop, *et al.*, "Optical technologies for terabit/s-throughput feeder link," *2017 IEEE International Conference on Space Optical Systems and Applications (ICSOS)*. (IEEE, 2017).
7. V. Spirito, G. Cossu, and E. Ciaramella, "Feasibility study of a Terabit/s GEO-to-Ground WDM Optical Communication Link," *Proc. SPIE, International Conference on Space Optics - ICSO 2022*.
8. R. E. Lafon, Y. Bai, A. Caroglanian, *et al.*, "NASA's Low-Cost Optical Terminal (LCOT) at Goddard Space Flight Center," *Proc. SPIE* **12413**, 124130 V (2023).

9. H. Kobayashi, R. Kano, T. Seo, *et al.*, "Development of a continuous wave single transverse mode polarization-maintaining 10 W Er/Yb-codoped fiber amplifier for space communications," SPIE Photonics West 2023.
10. D. Engin, S. Litvinovitch, C. Gilman, *et al.*, "50W, 1.5  $\mu\text{m}$ , 8 WDM (25 nm) channels PPM downlink Tx for deep space lasercom," *Proc. SPIE* **11272**, 112720 V (2020).
11. D. Engin, J. Hwang, P. Olmstead, *et al.*, "Experimental and theoretical study of TDM based FWM mitigation with 8 channel 50W WDM PPM Tx for slot sizes 0.5 and 1nsec," SPIE Photonics West, 2023, Paper 12413-14.
12. G. P. Agrawal, *Nonlinear fiber optics*, (Academic Press, 2001).
13. M. Shtaif, "Analytical description of cross-phase modulation in dispersive optical fibers," *Opt. Lett.* **23**(15), 1191–1193 (1998).
14. R. W. Tkach, A. R. Chraplyvy, F. Forghieri, *et al.*, "Four-photon mixing and high-speed WDM systems," *J. Lightwave Technol.* **13**(5), 841–849 (1995).
15. T. Anfray, P. Berceau, and L. Blarre, "Final report," Airbus Defence and Space, Toulouse, France, ESTEC Contract no 4000123012/18/UK/MM/gm techreport, FOLC.ADST.FR.001, Jul. 2019.
16. G. Cossu, A. Sgambelluri, F. Paolucci, *et al.*, "How Can Commercial Fiber Equipment Cope with the Random Fadings of FSO Links?" *Proceedings of European Conference on optical Communications, ECOC 2023*, P89.
17. D. A. Fishman and J. A. Nagel, "Degradations due to stimulated Brillouin scattering in multigigabit intensity-modulated fiber-optic systems," *J. Lightwave Technol.* **11**(11), 1721–1728 (1993).
18. C. J. Anderson and L. A. Lyle, "Technique for evaluating system performance using Q in numerical simulations exhibiting intersymbol interference," *Electron. Lett.* **30**(1), 71–72 (1994).
19. P. J. Winzer and R.-J. Essiambre, "Advanced optical modulation formats," *Optical Fiber Telecommunications VB*. (Academic Press, 2008). 23–93.
20. D. L. Fried, "Greenwood frequency measurements," *J. Opt. Soc. Am. A* **7**(5), 946–947 (1990).
21. E. Ciaramella and S. Trillo, "All-optical signal reshaping via four-wave mixing in optical fibers," *IEEE Photonics Technol. Lett.* **12**(7), 849–851 (2000).
22. E. L. Goldstein, L. Eskildsen, and A. F. Elrefaie, "Performance implications of component crosstalk in transparent lightwave networks," *IEEE Photonics Technol. Lett.* **6**(5), 657–660 (1994).
23. F. Forghieri, R. W. Tkach, and A. R. Chraplyvy, "WDM systems with unequally spaced channels," *J. Lightwave Technol.* **13**(5), 889–897 (1995).
24. M. P. Ninos, V. Spirito, G. Cossu, *et al.*, "Outage Performance of Uplink Pre-Amplified FSO Links Over Turbulence, Beam Wander, and Pointing Errors," *IEEE Commun. Lett.* **27**(12), 3275–3279 (2023).